Solid State Sciences 17 (2013) 90–96

Contents lists available at SciVerse ScienceDirect

Solid State Sciences

journal homepage: www.elsevier.com/locate/ssscie

Hydrothermal growth of $LiLuF_4$ crystals and new lithium lutetium fluorides $LiKLuF_5$ and $LiNaLu_2F_8$

Sara Comer, Colin D. McMillen, Joseph W. Kolis*

Department of Chemistry and Center for Optical Materials Science and Engineering Technologies (COMSET), Clemson University, Advanced Materials Research Laboratory, 91 Technology Drive, Anderson, SC 29625, USA

ARTICLE INFO

Article history:
Received 13 August 2012
Received in revised form
11 October 2012
Accepted 14 November 2012
Available online 1 December 2012

Keywords:
Hydrothermal synthesis
Lithium lutetium fluorides
$LiLuF_4$

ABSTRACT

The hydrothermal synthesis and crystal growth of $LiLuF_4$ were investigated. Small crystals of $LiLuF_4$ were produced but while investigating various alkali fluoride mineralizers, a new series of alkali lithium lutetium fluorides, including, $LiKLuF_5$ and $LiNaLu_2F_8$, were synthesized under hydrothermal conditions (570 °C at 12.5 kpsi). The mineralizer KF leads to formation of a new compound $LiKLuF_5$ crystallized in the space group $C2/m$ with the lattice parameters $a = 6.2328(12)$, $b = 11.709(2)$, $c = 6.3986(13)$, $\beta = 113.87(3)$. Tm and Yb analogs were also synthesized using the same conditions. Use of NaF as mineralizer leads to a new compound $LiNaLu_2F_8$, crystallized in space group $Cmcm$, $a = 10.3181(21)$, $b = 8.2393(16)$, $c = 6.9565(14)$. Several doped compounds were also isolated and electronic spectra were obtained.

1. Introduction

The use of metal fluorides as laser hosts presents several unique opportunities relative to the traditional oxides like YAG and YVO_4. Many of the fluorides melt at relatively low temperatures, making them potentially easier to grow. They can have low optical non-linearities, low thermal expansion and negative dn/dt values [1]. Fluorides especially have very wide transparency windows, with both high band edges and low IR absorption regions, often providing transparency ranges of 0.15–18 μm. The low IR absorption energy is particularly important for some lasing applications as it imparts very low phonon energy, which in turn, leads to long excited-state lifetimes. Thus 1% Nd^{3+} has a lifetime of 240 μs in YAG and 98 μs in YVO_4, but over 500 μs in $LiYF_4$ (YLF) for its 1.06 micron emission [1].

Long fluorescence lifetimes enable a number of optical effects caused by multiple photon absorption, such as upconversion, which is the absorption of two or more pump photons to a higher energy level. Subsequent emission from these higher levels produces shorter wavelength light than the pump wavelength. Thus upconversion can replace second harmonic generation as a process to convert readily available IR diode pump wavelengths to desirable visible or UV emission using only one crystal [2,3]. This can ultimately lead to cheap, compact visible emission display devices.

The most common metal fluoride host is $LiYF_4$ and it has received considerable study [4–6] along with its analog $LiLuF_4$ [5,7–9]. The use of lutetium in place of the more common yttrium ion host is of interest because it leads to a better match of size and mass in the lattice with the heavier rare earths like Yb, Er and Tm. $LiLuF_4$ also melts congruently and has some physical characteristics superior to YLF. The use of Lu as a host ion can also result in subtle spectroscopic differences when compared to analogous Sc, Y, La or Gd based compounds. In general the fluorides probably have not received as much attention as the oxides as host materials. Another particularly unusual class is the mixed alkali $LiKMF_5$. Previous work focused on the parent $LiKYF_5$ and to a lesser extent, its Gd analog [10–15] reveals a series of interesting structural anomalies. Given the potential significance of metal fluorides as optical hosts and the interesting complexity of this particular system as well as our long-standing interest in hydrothermal growth single crystal for optical applications [16–19], we initiated an investigation into the hydrothermal chemistry of various metal fluorides [20,21].

In particular we began the investigation of the hydrothermal growth of $LiLuF_4$ single crystals. We find that it is indeed possible to grow $LiLuF_4$ single crystals hydrothermally but they have not yet grown well. We find that LiF is not an optimal mineralizer because the low solubility of the material prevents use of sufficient concentration of mineralizer to lead to large crystal growth, so a more systematic investigation of the alkali metals was

* Corresponding author.
E-mail address: kjoseph@clemson.edu (J.W. Kolis).

1293-2558/$ – see front matter © 2012 Elsevier Masson SAS. All rights reserved.
http://dx.doi.org/10.1016/j.solidstatesciences.2012.11.019

undertaken. The fluorides NaF and KF led to a series of new phases unique to lutetium including $LiNaLu_2F_8$ and $LiKLuF_5$. Use of RbF and CsF did lead to larger crystals of $LiLuF_4$ with no inclusion of the larger alkali ion in the structure. The structures and some preliminary spectroscopy of this subtle and interesting system are presented herein.

2. Experimental procedure

2.1. Hydrothermal synthesis

Hydrothermal phase space in these systems was explored by the reaction of various powdered starting materials with an aqueous mineralizer in weld-sealed silver ampoules. Sealed ampoules were then placed in an autoclave and the remaining volume of the autoclave was filled with deionized water to serve as counter pressure. The autoclave was heated to 550–600 °C, typically generating 10–20 kpsi pressure. The crystalline products were harvested from the ampoules after the autoclave was cooled to room temperature. Crystals of $LiLuF_4$ (LLF) were obtained both by the reaction of LiF and LuF_3 under hydrothermal conditions and hydrothermal recrystallization of LLF powder. The approach that produced the best crystalline LLF product in phase pure yields was to first make a polycrystalline melt of LLF, then recrystallizing the LLF by a hydrothermal treatment. The solid-state melt product was prepared using LiF (Aldrich, ≥99.98%) and LuF_3 (Alfa Aesar, 99.9%) in a molar ratio of 1:1. These were mixed intimately and heated in a platinum crucible for 900 °C for 12 h under flowing N_2. The resulting LLF powder, 0.1 g, was then sealed in a silver ampoule with aqueous CsF (2 M, 0.4 mL) and was treated hydrothermally at 590 °C for 6 d at 12 kpsi.

Crystals of $LiKLuF_5$ (1) and $LiNaLu_2F_8$ (2) were similarly obtained using a two-step procedure. In both cases polycrystalline LLF powder was first prepared from the solid-state reaction described above. Compound (1) was then formed using hydrothermal reactions in silver ampoules with aqueous KF (3 M, 0.4 mL) as a mineralizer with 0.1 g of $LiLuF_4$. The reactions were performed at 570 °C and 12.5 kpsi for 6 d. Crystals of $LiKLuF_5$ formed as colorless rod-like crystals up to 6 mm in size. A small colorless crystal $0.20 \times 0.20 \times 0.20$ mm^3 in size was selected for single crystal diffraction. Compound (2) was prepared using hydrothermal techniques in a sealed silver ampoule at 590 °C and 22 kpsi for 14 days. The LLF starting material (0.1 g) was added to the ampoules along with an aqueous solution of NaF (3 M, 0.4 mL) as a mineralizer. A small colorless crystal was removed for single crystal diffraction that was $0.20 \times 0.20 \times 0.16$ mm^3 in size. Crystals of (1) and (2) were also doped with the rare earth ions Nd^{3+} and Tm^{3+}. These crystals were prepared through a hydrothermal reactive process where LiF, LuF_3 and the dopant fluoride, NdF_3 (Aldrich, 99.99%) and TmF_3 (Alfa Aesar, 99.9%) were combined in the desired ratio and mineralized with NaF or KF. Various crystals are shown in Fig. 1.

For comparison of the phase space and evaluation of structural trends the study was extended to include crystals of other complex fluorides based on the rare earth elements Y, Ho, Tm and Yb. These systems were likewise explored by the hydrothermal reaction of component fluorides as well as hydrothermal recrystallization of polycrystalline starting materials using various mineralizers. Reaction products were characterized by X-ray diffraction and optical absorption techniques. Bulk phase identification was achieved using a Rigaku Ultima IV powder diffractometer utilizing Cu Kα radiation ($\lambda = 1.5418$ Å). Finely ground samples were scanned from 5 to 65° in two-theta at a rate of 1°/min in 0.02° intervals. The structures of (1) and (2) were determined by single crystal X-ray diffraction as described below. Absorption spectra were collected on single crystals or pressed pellets of Nd^{3+}:$LiKLuF_5$, $LiKYbF_5$, $LiKTmF_5$ and Tm:$LiNaY_2F_8$ using a Perkin Elmer Lambda 900 UV/Vis/NIR Spectrometer to confirm rare earth doping or full substitution where applicable. Data were collected at a rate of 0.9 nm/s.

2.2. Crystal structure determination

A summary of the crystallographic data for the new compounds $LiKLuF_5$ (1) and $LiNaLu_2F_8$ (2) is provided in Table 1. A single crystal of each compound was mounted on a glass fiber with epoxy. Single crystal diffraction was performed on each of the crystals using a Rigaku AFC8S diffractometer with a Mercury CCD detector and a graphite monochromated Mo radiation source ($\lambda = 0.70926$ Å). Data were corrected for absorption and Lorentz and polarization effects using the CrystalClear software package [22]. The structures were determined by direct methods followed by subsequent refinement using full-matrix least-squares techniques using the SHELXTL software package [23]. The structure of $LiKLuF_5$ was determined in space group $C2/m$ based on the systematic absences of the data. All atoms were refined anisotropically. A final R_1 value of 0.043 was obtained for 1894 total reflections, 459 of which were unique. Attempts to determine the structure in space group $P2_1/c$, according to a previously reported structure for $LiKYF_5$, were unsuccessful, as the R_1 value for this test case was 0.197 and the atoms exhibited unacceptable anisotropic displacement parameters [11,12]. Likewise the structure of $LiNaLu_2F_8$ was determined in the orthorhombic space group $Cmcm$ based on the systematic absences. After anisotropic refinement a final R_1 value of 0.045 was obtained for 2631 total reflections (348 unique reflections). Attempts to solve this structure in space group $P2_1/m$, as reported for $LiNaY_2F_8$, were not successful [24].

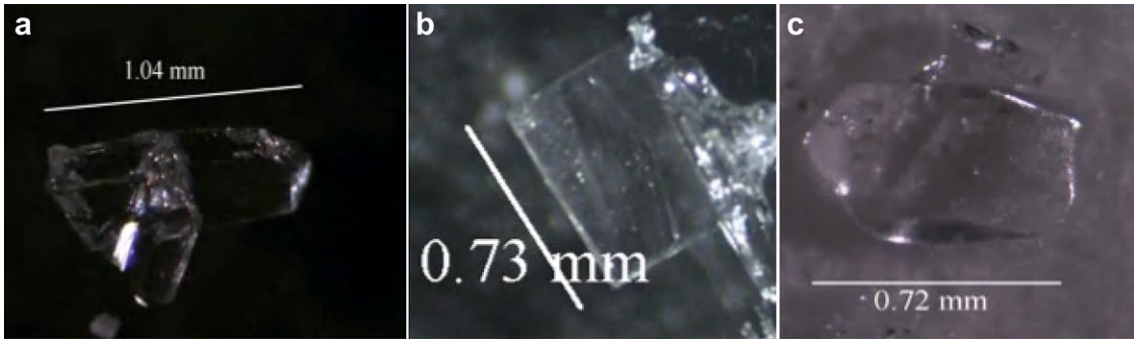

Fig. 1. Images of (a) $LiKLuF_5$, (b) $LiNaLu_2F_8$, (c) $LiLuF_4$.

Table 1
Crystallographic data of novel complex lutetium fluorides.

	(1)	(2)
Empirical formula	$LiKLuF_5$	$LiNaLu_2F_8$
Formula weight	316.01	1123.60
Space group	*C*2/*m*	*Cmcm*
a, Å	6.2328(12)	10.3181(21)
b, Å	11.709(2)	8.2393(16)
c, Å	6.3986(13)	6.9565(14)
β, °	113.87(3)	
V, Å^3	427.05(15)	591.4(2)
Z	4	4
D_{calc}, Mg/m^3	4.915	5.974
Parameters	48	39
μ, mm^{-1}		33.365
θ range, °	3.48–26.29	3.16–26.33
Reflections		
Collected	1894	2531
Independent	456	348
Observed	452	348
R (int)	0.0720	0.1254
Final R (obs. data)[a]		
R_1	0.0432	0.0454
wR_2	0.1047	0.1146
Final R (all data)		
R_1	0.0433	0.0454
wR_2	0.1048	0.1146
Goodness of fit on F^2	1.139	1.097
Largest diff. peak, e/Å^3	4.17	3.202
Largest diff. hole, e/Å^3	−3.67	−4.519
Measurement temperature (K)	293	293

[a] $R_1 = [\sum||F_0| - |F_c||]/\sum|F_0|$; $wR_2 = \{[\sum w[(F_0)^2 - (F_c)^2]^2]\}^{1/2}$.

3. Results and discussion

3.1. Reactions and synthesis

A reaction summary highlighting the important reaction conditions and products in this study is shown in Table 2. Our original goal in this work was to develop a hydrothermal route to single crystals of $LiLuF_4$ (LLF), which is a considerably less well-known system than $LiYF_4$. We found that both YLF and the $LiLuF_4$ analogs do indeed form in hydrothermal conditions. YLF was formed using a solid-state reaction to make a melt and then given a hydrothermal treatment with CsF as a mineralizer. The technique is similar to all others reported in this paper. However, because the chemistry of $LiLuF_4$ is so much less known we chose to focus on that topic. The effects of the alkali fluoride mineralizers used are given in Table 2. While LLF can be crystallized using several different mineralizers we find some to be more preferable than others. Perhaps somewhat surprisingly we find that LiF does not provide satisfactory transport and growth of large crystals of $LiLuF_4$ because of the relative insolubility of LiF. The use of higher LiF concentrations only seems to encourage the crystallization of larger LiF crystals rather than LLF.

Table 2
Reaction conditions and products.

Reaction	Starting materials	Mineralizer	Products
A	LiF, LuF_3	DI H_2O	$LiLuF_4$
B	LiF, LuF_3	1 M LiF	LiF, $LiLuF_4$
C	LiF, LuF_3	1 M KF	$LiLuF_4$
D	$LiLuF_4$	DI H_2O	$LiLuF_4$
E	$LiLuF_4$	1 M LiF	LiF, $LiLuF_4$
F	$LiLuF_4$	0.5 M KHF_2	$LiLuF_4$
G	$LiLuF_4$	1 M CsF	$LiLuF_4$
H	$LiLuF_4$	2 M CsF	$LiLuF_4$
I	$LiLuF_4$	2 M RbF	$LiLuF_4$,
J	$LiLuF_4$	2 M NaF	$LiLuF_4$, $NaLuF_4$
K	$LiLuF_4$	3 M NaF	$LiNaLu_2F_8$
L	$LiLuF_4$	3 M KF	$LiKLuF_5$

Thus we began exploring the other alkali metal fluoride mineralizers NaF and KF, which have greater solubility in supercritical water. We find that these two mineralizers introduce additional alkali metal ions that become incorporated into the lattice of the lutetium fluorides leading to a series of new compounds containing two heterogeneous alkali metal ions. It is somewhat interesting that the mixed alkali lutetium fluoride, $LiNaLu_2F_8$ (2), only forms from higher NaF concentrations, whereas the simpler, sodium-richer $NaLuF_4$ phase was synthesized at lower NaF concentrations [25]. Under similar conditions KF mineralizers showed a marked tendency toward the formation of $LiKLuF_5$ (1), and phase pure yields of the rod-like crystals could be obtained.

In both cases the resultant structures are different from those of the yttrium compounds with similar formulas (vide infra). Returning to the original thesis that the more-soluble alkali fluoride mineralizers would be useful in crystallizing $LiLuF_4$ we explored RbF and CsF mineralizers. Indeed we found these to be the most suitable for the recrystallization of LLF, as the mineralizer does not recrystallize in the hydrothermal fluid, and no heterogeneous mixed alkali lutetium fluorides were formed. Under optimum conditions explored in this study using a 2 M CsF mineralizer LLF crystals up to 1.0 mm in size were obtained. An interesting effect we discovered was the when using starting materials of LuF_3 and LiF instead of a melt starting material we get the desired $LiLuF_4$ along with crystallization of the mineralizer, excepting DI H_2O. It was decided to move to a starting material made from a melt material of $LiLuF_4$ and we then attempted to crystallize it using hydrothermal techniques.

In both cases of the new heterogeneous alkali lutetium fluorides we find that is it easy to grow various lanthanide doped analogs simply by using a hydrothermal reaction of the correct molar ratio of powder LuF_3, LiF, and the appropriate dopant materials (LnF_3) while using either NaF or KF as a mineralizer. We also find that in case of the potassium compound 1 the smaller heaviest lanthanides (Yb, Tm) also grow as isostructural analogs to $LiKLuF_5$ in phase pure yields. This trend appears to discontinue when the larger Ho^{3+} ion is used, and the known KHo_2F_7 is the preferred product [15].

3.2. Structure of $LiKLuF_5$

The structure of $LiKLuF_5$ (1) was determined in the monoclinic space group *C*2/*m* with unit cell parameters of $a = 6.2328(12)$ Å, $b = 11.7093(23)$ Å, $c = 6.3986(13)$ Å, and $\beta = 113.87(3)^\circ$. Selected bond distances and angles are given in Table 3. The unit cell of the $LiKLuF_5$ structure is shown in Fig. 2a. The structure of (1) contains eight-coordinate Lu atoms on a special position with mirror symmetry. Lu–F bonds range in length from 2.167(18)–2.303(12) Å. These lutetium fluoride polyhedra propagate by edge sharing with one another, ultimately forming layers perpendicular to [010] with elongated hexagonal gaps as shown in Fig. 2b. The gap pattern in a given layer is staggered with respect to the next layer along the *b*-axis, preventing the formation of channels. Even so, the potassium atoms are aligned with these gaps and sit above and below the Lu–F layers on a 2-fold symmetry site. The potassium ion is eight-coordinate with fluorine and typical K–F bond distances ranging from 2.634(9)–2.849(11) Å are observed. Two longer contacts to F1 atoms exist at 3.49 Å from the potassium atom, but since its bond valence is satisfied with the existing eight normal contacts these probably should not be considered bonds. Lithium atoms are half-occupied at a general position and are four-coordinate with fluorine forming a distorted tetrahedron. Li–F bond distances range from 1.80(6)–2.14(4) Å. Lithium atoms reside between the lutetium fluoride layers and serve to connect the layers along the *b*-axis by both edge and corner sharing. As a result the lithium lutetium

Table 3
Selected bond distances (Å) and angles (°) for $LiKLuF_5$.

$LiKLuF_5$ (1)		$LiNaLu_2F_8$ (2)	
Distances		*Distances*	
Lu1–F2	2.161 (12)	Lu1–F2	2.181 (8)
Lu1–F3	2.185 (10)	Lu1–F2	2.184 (8)
Lu1–F4	2.219 (8) (×2)	Lu1–F4	2.192 (8)
Lu1–F2	2.252 (12)	Lu1–F1	2.199 (6) (×2)
Lu1–F1	2.268 (5) (×2)	Lu1–F1	2.275 (6) (×2)
Lu1–F3	2.299 (10)	Lu1–F3	2.392 (7)
Li1–F1	1.78 (4)	Li1–F3	1.893 (5) (×2)
Li1–F4	1.85 (5)	Li1–F1	2.262 (7) (×4)
Li1–F4	1.86 (4)		
Li1–F4	2.14 (4)	Na1–F4	2.167 (18)
		Na1–F1	2.313 (7) (×4)
K1–F3	2.631 (8) (×2)	Na1–F4	2.510 (10) (×2)
K1–F4	2.669 (10) (×2)		
K1–F2	2.724 (10) (×2)	*Angles*	
K1–F4	2.849 (9) (×2)	F3–Li1–F3	180.0 (7)
		F1–Li1–F3	81.2 (3)
Angles		F1–Li1–F3	98.8 (3)
F1–Li1–F4	109 (2)		
F1–Li1–F4	83 (1)		
F1–Li1–F4	108 (2)		
F4–Li1–F4	121(2)		

fluoride network forms cages within which the potassium atoms sit.

Isostructural compounds $LiKYbF_5$ (a = 6.2583(13) Å, b = 11.720(2) Å, c = 6.4045(13), and β = 113.83(3)°) and $LiKTmF_5$ (a = 6.2907(13) Å, b = 11.744(2) Å, c = 6.4374(13) Å, β = 114.05(3)°) were identified when the phase space was expanded to study other rare earth metals.

Previous work with the yttrium compound having the same formula, $LiKYF_5$, revealed some subtle and unusual structural aspects. The crystals grow in a slightly different structure depending on the method of growth. Thus $LiKYF_5$ crystallizes in the space group $P2_1/c$ regardless of whether it is grown by a Czochralski (CZ) melt pulling technique or a hydrothermal method. It crystallizes in a different space group, $P2_1/c$, though having similar lattice parameters to the $LiKLuF_5$ analog; a = 6.2925(4) Å, b = 11.747(1) Å, c = 6.4669(5) Å, β = 113.715(6)° [10]. However, the CZ growth of $LiKYF_5$ leads to a unit cell that is twice as large as the hydrothermally grown crystals because it is exactly doubled along the b-axis. The result of that doubling is that there are twice as many unique metal center sites in the CZ grown crystal. The metal sites are low symmetry in all cases with no inherent crystallographic symmetry in their coordination environment.

The presence of a larger unit cell with two different types of metal coordination environments in the lattice manifests itself in a number of ways. The powder patterns of the two structural types are slightly different and most importantly, the spectroscopy is different. In particular the photoluminescence spectrum of the CZ grown material has essentially a series of "doublets" in the 1047 nm region relative to the hydrothermally grown product, suggesting that emission is coming from two generally similar but slightly different metal sites. Careful spectroscopic study of Nd^{3+} doped materials indicates that both sites are occupied in equal proportion [13]. In addition the multiple sites also lead to a broadening of the absorption peaks due to the multiple low symmetry sites. Broad absorption bands are often useful for solid-state laser actions, particularly if diode lasers are used for pumping because the demands for careful control of diode pump wavelength can be relaxed somewhat with broad absorption bands. Broad emission is also useful for ultrafast lasing [18].

Interestingly in the case of $LiKLuF_5$ we find that the Lu containing crystals grown hydrothermally possess the same unit cell dimensions as the small Y analog but the structure is different. The structures of primitive $LiKYF_5$ and C-centered $LiKLuF_5$ are compared in Fig. 3. Both structures have a similar rare earth fluoride network and thus have a related layered structure. The unit cell is C-centered with $C2/m$ symmetry, in contrast to the primitive unit cells of $LiKYF_5$. In addition the lanthanide metal sits on a higher symmetry site. Thus there are two metal sites in the unit cell but they are crystallographically identical. We find that the Yb and Tm analogs can be prepared as well with $C2/m$ symmetry, but that the structure reverts back to the primitive lattice type as the larger lanthanides are used (Ho and larger).

In the lutetium compound however the lithium atoms are more distorted in their bonds to fluorine, and the layers are not as extensively connected. Perhaps resulting from this, potassium atoms occupy a different relative location in the lattice and their local environment is notably different between the structure types. In the $LiKYF_5$ structure K^+ is in a 9 coordinate distorted environment. The K–F bond distances range in length with eight bonds from 2.65–2.90 Å and one longer contact at 3.11 Å. As discussed earlier the new $LiKLuF_5$ structure has eight-coordinate K–F bonds ranging in length from 2.63(1)–2.84(3) Å with two very long contacts at 3.49 Å that are not considered to be bonds because the bond valence of the K atom is already satisfied. This difference in potassium coordination results in only three Li–F–K bridges being formed from the LiF_4 tetrahedra in $LiKLuF_5$ as opposed to four Li–F–K bridges occurring in $LiKYF_5$. Since $LiKYF_5$ crystallizes in the

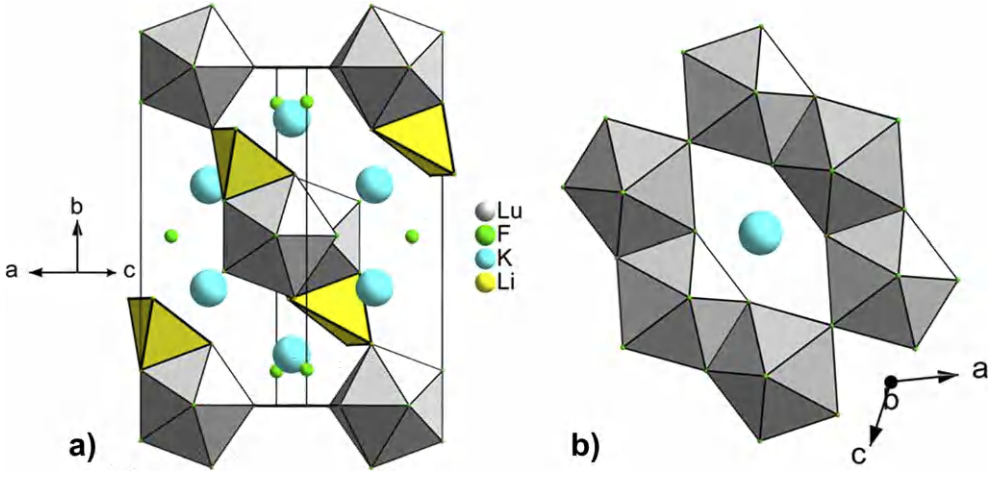

Fig. 2. a) Unit cell of $LiKLuF_5$ viewed along [001]. b) Hexagonal gaps in a single lutetium fluoride layer viewed along [010].

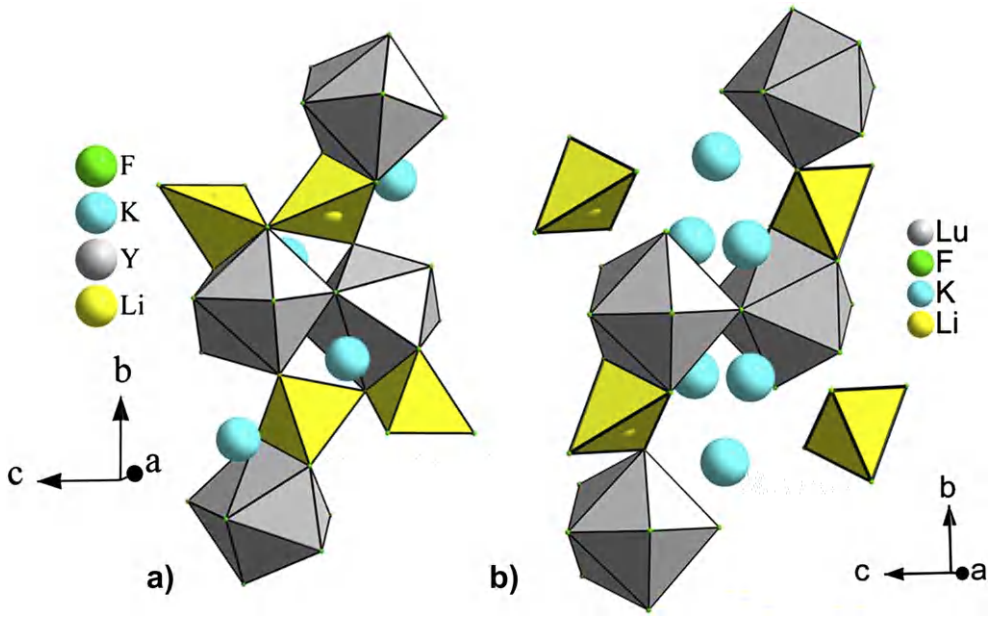

Fig. 3. Comparison of $LiKYF_5$ (left), and $LiKLuF_5$ (right) materials.

primitive lattice type and the larger holmium ions form KHo_2F_7, we propose that crystallization in the *C*-centered lattice type may occur as a function of the ionic radius of the rare earth ion. In our study all the *C*-centered structures have rare earth ions with eight-coordinate crystal radii smaller than 1.14 Å. Alternatively, eight-coordinate Ho^{3+} and Y^{3+} have crystal radii of 1.16 Å [26]. While the rare earth fluoride network itself does not appear to change the smaller rare earth ions perhaps drive the structures to differ by causing distortion about the lithium ions and rearrangement of the potassium ions. A comparison of the powder X-ray patterns in Fig. 4 indicates the Lu, Yb and Tm analogs are isostructural, but do not exhibit the subtle peaks present in the Y-based compound.

3.3. Structure of $LiNaLu_2F_8$

The crystal of $LiNaLu_2F_8$ was solved in the orthorhombic space group *Cmcm*. The unit cell parameters are $a = 10.3181(21)$ Å, $b = 8.2393(16)$ Å, and $c = 6.9565(14)$ Å. The lutetium atoms are again eight-coordinate with mirror symmetry, having similar

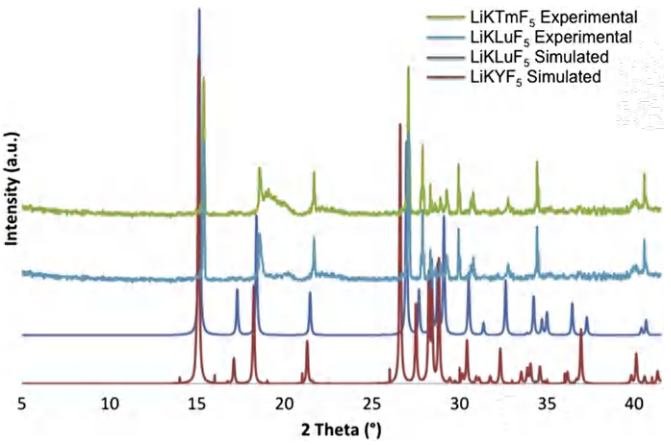

Fig. 4. Powder patterns for $LiKLnF_5$ materials.

fluoride bond distances to (1) and other rare earth fluorides (Table 3). These LuF_8 polyhedra connect by edge sharing to form layers perpendicular to [010]. These layers are staggered with respect to one another and connected along [010] by Lu–F–Lu corner sharing resulting in a three-dimensional Lu–F framework (Fig. 5a). The individual layers exhibit hexagonal gaps in the framework, which accommodate the sodium atoms (Fig. 5b). The Na atoms are seven coordinate and have square face monocapped trigonal prismatic geometry, and they sit on *m*2*m* symmetry sites. Sodium atoms fit snugly between the lutetium atoms and share fluoride edges and corners with the LuF_8 polyhedra. Na–F bonds vary in length from 2.166(18)–2.510(10) Å. The somewhat short Na1–F4 bond is nearly aligned along the *b*-axis and is part of a shared edge with Lu1 and F2. The Na1–F2 bond happens to be the longest of the observed Na–F bonds. LiF_6 octahedra form chains that propagate along the *c*-axis by Li–F–Li corner sharing. The two shorter Li–F bonds are along the axial positions of the LiF_6 polyhedra. It is the shorter Li1–F3 bonds that propagate the chains which are bound by the Na–Lu–F framework. The longer Li1–F1 bonds make edge sharing connections to edges of the square face of the NaF_7 polyhedron. Thus the sodium atoms are isolated from one another in cages formed by the LuF_8 and LiF_6 polyhedra (Fig. 5).

Alternatively, the previously published yttrium analog of this compound, $LiNaY_2F_8$ is reported in the monoclinic space group $P2_1/m$ with the cell parameters of $a = 6.6220$ Å, $b = 6.9950$ Å, $c = 6.6320$ Å, and a beta angle of 103.14° [24]. Also, a previous study on the structure of $LiNaYb_2F_8$ reported *C*-centered monoclinic symmetry (s.g. $C2/c$) with pseudo-orthorhombic symmetry [27]. Other reports from powder X-ray data indicate the lanthanide analogs crystallize in space group $P2_1/m$ like the yttrium compound [28]. Thus a degree of ambiguity exists in the literature. Examination of the structures of hydrothermally grown $LiNaLu_2F_8$ as grown here and the primitive monoclinic $LiNaY_2F_8$ (grown by solid-state techniques) indicates some similarity in the structures. Equivalent orientations can be observed when viewed along [010] in the orthorhombic structure and [101] in the monoclinic structure. The difference in the two structures arises from the presence of two unique yttrium sites in monoclinic $LiNaY_2F_8$ and only one unique lutetium site in (2). Even in the monoclinic compound the unique

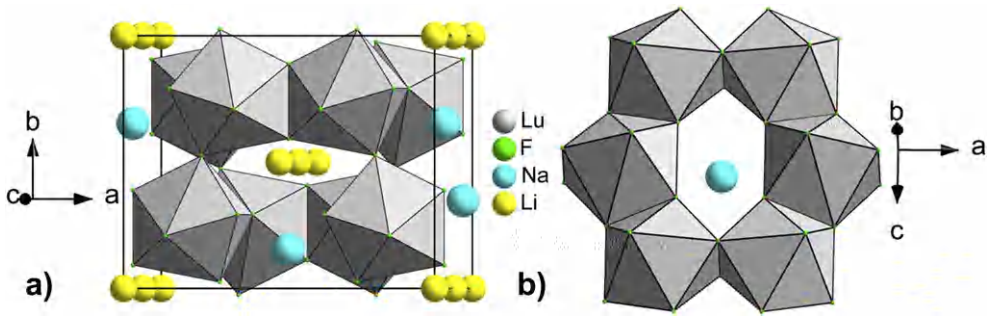

Fig. 5. a) Unit cell of $LiNaLu_2F_8$. b) Individual layer of edge sharing LuF_8 polyhedra.

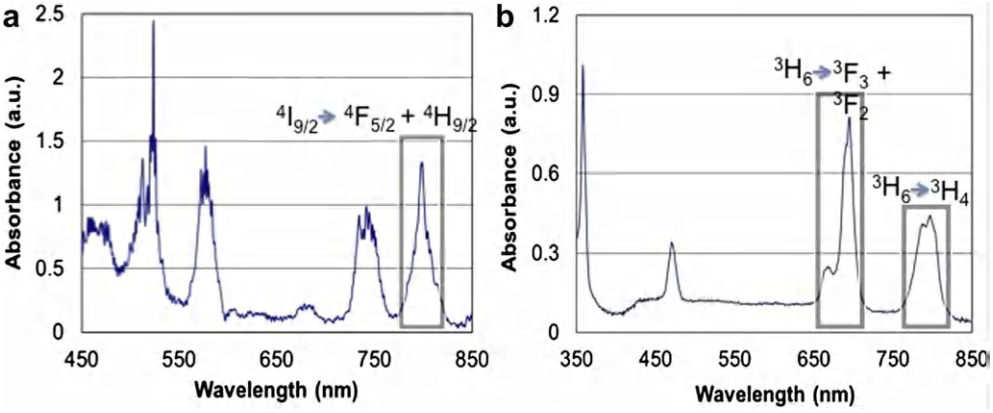

Fig. 6. UV/vis absorption spectrum for (a) Nd:$LiKLuF_5$ and (b) Tm:$LiNaLu_2F_8$. The key absorption bands for common optical applications are highlighted.

sites differ only slightly and give the appearance of pseudo-orthorhombic symmetry. It is possible that hydrothermal growth at lower temperatures mediates these subtle differences in site symmetry, making the orthorhombic symmetry more apparent in the systematic absences of the data. For the Lu compound there are LuF_8 polyhedra that have varying bond distances from 2.1808 to 2.3898 Å. For the YF_8 polyhedra there are two unique Y sites. The Y1 site has varying bond distances from 2.183 to 2.411 Å while the Y2 site has bond distances from 2.185 to 2.419 Å. Similarities in these Y sites contribute to the pseudo-orthorhombic symmetry observed in the Y and Yb compounds [27], and the similarities to the Lu site in the orthorhombic $LiNaLu_2F_8$ is evident. To our knowledge the present work represents the first full structure refinement assuming orthorhombic symmetry.

3.4. Absorption spectroscopy

Despite numerous attempts we are not yet able to get sufficiently large single crystals to obtain high-resolution electronic spectra so we were forced to use translucent pressed pellets for absorption data which resulted in somewhat broadened absorption peaks. However the spectra are sufficient to identify the typical peaks and confirm the presence of dopant ions and their approximate electronic spectra in these hosts. Spectroscopy was used to observe the transitions in the compounds $LiKTmF_5$ and $LiKYbF_5$ as well as the Nd^{3+} doped Nd:$LiKLuF_5$ in which the Nd^{3+} ion is doped into the Lu^{3+} site (Fig. 6a). For 5% Nd:$LiKLuF_5$ the absorption band for $^4I_{9/2}$ to $^4F_{5/2} + {}^2H_{9/2}$ typically observed at 808 nm in crystal systems like YAG is observed here at 799 nm. This is comparable to what is observed in Nd:$LiKYF_5$ [11].

Absorption spectra for Tm doped $LiNaY_2F_8$ were also measured in Fig. 6, again using a translucent pressed powder resulting in some loss of resolution. They are generally similar to other Tm doped materials and serve to demonstrate that material can be readily doped with f elements using hydrothermal methods. The spectrum of the Tm^{3+} doped material has significant peaks located at 650–707 nm corresponding to transitions from the ground state $^3H_6$ to excited $^3F_3 + {}^3F_2$ states. The peak located at 350 nm corresponds to the $^3F_4$ to the $^1D_2$ transition and has been reported to be useful in upconversion processes to generate a blue emission at 453 nm [22]. The band located at 800 nm corresponds to the $^3H_6$ to $^3H_4$ transition. All the peaks shown in Fig. 6 are characteristic for Tm^{3+} absorption in materials such as Tm:YLF and Tm:YVO_4 [29]. In addition the optical windows for undoped and doped materials were found. All materials were optically transparent from 250 to 2000 nm, the limits of the instrument used.

4. Conclusions

The paper reports the preliminary chemical investigation of $LiLuF_4$ in hydrothermal fluids. We find that $LiLuF_4$ can be grown as phase pure single crystals in hydrothermal fluids. They are not yet of sufficiently high quality for laser applications due in part to the inability to employ higher concentrations of LiF as a mineralizer because of its low solubility in hydrothermal fluids. Because of this we investigated the other alkali fluorides as mineralizers. We found that both RbF and CsF mineralizers lead to improved growth of $LiLuF_4$ crystals.

When the smaller alkali fluorides KF and NaF are used, the alkali metal ions become incorporated in the final product and several new compounds are isolated. Herein we report the growth, structure properties, and spectroscopy of novel fluoride crystals of $LiKLuF_5$, as well as several other analogs such as $LiKYbF_5$. These compounds crystallize in a *C*-centered monoclinic system. Crystals

of these compounds were produced in sizes ranging from 0.20 mm up to 6 mm. These crystals were grown hydrothermally using 3 M KF as a mineralizer at a temperature of 570 °C and were produced in good yield. The use of NaF as a mineralizer resulted in the isolation of a new phase $LiNaLu_2F_8$. Crystalline powder and single crystals were produced up to 0.20 mm in size. The analogous yttrium compound is reported to crystallize in the monoclinic crystal system, but having pseudo-orthorhombic symmetry, whereas the present study on $LiNaLu_2F_8$ refines the structure based on full orthorhombic symmetry. Rare earth doping was demonstrated in both $LiKLuF_5$ and $LiNaLu_2F_8$ systems, and the absorption spectra of Nd^{3+} and Tm^{3+} doped compounds are reported. The spectra are similar to those of other rare earth doped complex fluorides. Further studies are underway to determine the potential optical properties of these novel compounds and optimize the growth of high quality single crystals of $LiLuF_4$ for use as an optical host material.

Acknowledgments

We are grateful to the National Science Foundation for financial support of this work (Grant #DMR-0907395).

References

[1] Y. Kalisky, The Physics and Engineering of Solid State Lasers, SPIE Press, Bellingham, 2006, pp. 43–65 (Chapter 5).
[2] H. Scheif, G. Huber, E. Heuman, S. Bär, E. Osiac, Opt. Mater. 26 (2004) 365–374.
[3] M.F. Joubert, Opt. Mater. 11 (1999) 181–203.
[4] A.L. Harmer, A. Linz, D.R. Gabbe, J. Phys. Chem. Solids 30 (1969) 1483–1491.
[5] E.J. Sharp, D.J. Horowitz, J.E. Miller, J. Appl. Phys. 44 (1973) 5399–5401.
[6] N.P. Barnes, B.M. Walsh, K.E. Murray, G.J. Quarles, V.K. Castillo, J. Opt. Soc. Am. B 15 (1998) 2788–2793.
[7] A. Bensalah, Y. Guyot, A. Brenier, H. Sato, T. Fukuda, G. Boulon, J. Alloys Compd. 380 (2004) 15–26.
[8] C. Znoa, L. Zhang, Y. Hang, X. He, J. Yin, P. Hu, G. Chen, M. He, H. Huang, Y. Zhu, J. Phys. D: Appl. Phys. 43 (2010) 495403–495409.
[9] N.P. Barnes, B.M. Walsh, K.E. Murray, G.J. Quarles, V.K. Castillo, OSA Trends Opt. Photonics Ser. 10 (1997) 448–450.
[10] A.V. Goryunov, A. Popov, N.M. Khaidukov, P.P. Fedorov, Mater. Res. Bull. 27 (1992) 213–220.
[11] A.A. Kaminskii, V.S. Mironov, S.N. Bagalev, N.M. Khaidukov, M.F. Joubert, B. Jaquier, G. Boulon, Phys. Stat. Sol. (a) 145 (1994) 177–195.
[12] A.A. Kaminskii, V.S. Mironov, S.N. Bagaev, G. Boulon, N. Djeu, Phys. Stat. Sol. (b) 185 (1994) 487–504.
[13] H. Weidner, W.A. McClintic, M. McKaig, B.H.T. Chai, R.E. Peale, OSA Proc. Adv. Solid State Lasers 24 (1995) 545–550.
[14] J.F.H. Nicholls, X.X. Zhang, M. Bass, B.H.T. Chai, B. Henderson, Opt. Commun. 137 (1997) 281–284.
[15] A. Smith, J.P.D. Martin, M.J. Sellars, N.B. Manson, A.J. Silversmith, B. Henderson, Opt. Commun. 188 (2001) 219–232.
[16] C.D. McMillen, J.W. Kolis, J. Cryst. Growth 310 (2008) 1939–1942.
[17] A.R. Forbes, C.D. McMillen, H.G. Giesber, J.W. Kolis, J. Cryst. Growth 310 (2008) 4472–4476.
[18] C. Honninger, et al., Appl. Phys. B 69 (1999) 3–17.
[19] Y. le Fur, S. Aleonard, M.F. Gorius, M.T. Roux, Acta Crystallogr. B 38 (1982) 1431–1436.
[20] K. Shimamura, H. Sato, et al., Cryst. Res. Technol. 36 (2001) 801–813.
[21] C. McMillen, J. Kolis, Philos. Mag. 92 (2012) 2686–2711.
[22] Molecular Structure Corporation & Rigaku, CrystalClear, Version 1.3, Rigaku Corporation/MSC, Tokyo, Japan/The Woodlands, TX, USA, 2000.
[23] G.M. Sheldrick, Acta Crystallogr. A 64 (2008) 112–122.
[24] D. Avignant, D. Zambon, et al., Rev. Chim. Miner. 21 (1984) 771–777.
[25] Brunton, et al. Oak Ridge Natl. Lab. Rep. (U.S.) 3761 (1965).
[26] R. Shannon, C. Prewitt, Acta Crystallogr. B 25 (1969) 925.
[27] A. Dib, M.F. Gorius, S. Aleonard, J. Solid State Chem. 65 (1986) 205–214.
[28] D. Zambon, J. Metin, B. Picaud, D. Avignant, C. R. Acad. Sci. Paris Ser. 2 301 (1985) 1235.
[29] L.C. Courrol, I.M. Ranieri, S.L. Baldochi, et al., Opt. Commun. 270 (2007) 340–346.